Development of Flexible Structural Precast Concrete Conduits for Earth Dams

Sawada, Yutaka
Arita, Junichi
Omori, Masaki
Ariyoshi, Mitsuru
Kawabata, Toshinori

(Citation)
Journal of Pipeline Systems Engineering and Practice,13(1):04021073

(Issue Date)
2021-10-15

(Resource Type)
journal article

(Version)
Accepted Manuscript

(URL)
https://hdl.handle.net/20.500.14094/0100480891

Development of flexible structural precast concrete conduits for earth dams

Yutaka Sawada[1]*, Junichi Arita[2], Masaki Omori[3], Mitsuru Ariyoshi[4], and Toshinori Kawabata[5]

[1] Associate Professor, Graduate School of Agricultural Science, Kobe University,
1-1 Rokkodaicho, Nada-ku, Kobe-shi, Hyogo 657-8501, Japan. sawa@harbor.kobe-u.ac.jp
[2] Deputy General Manager, Technology Div., Vertex Corp., 9F Shin-Osaka 1st MT Bldg., 5-13-9
Nishinakajima, Yodogawa-ku, Osaka-shi, Osaka
532-0011, Japan.
ju-arita@vertex-grp.co.jp
[3] Chief, Dept. of Engineering, Daiwa Cres Co. Ltd., 2-7-34 Fujiwaranishimachi, Naka-ku, Okayama-shi,
Okayama 703-824, Japan.
masaki.oomori@daiwa-cres.co.jp
[4] Senior Researcher, Institute for Rural Engineering, NARO,
3-1-1 Kannondai, Tsukuba-shi, Ibaraki 305-8517, Japan. ariyoshi@affrc.go.jp
[5] Professor, Graduate School of Agricultural Science, Kobe University,
1-1 Rokkodaicho, Nada-ku, Kobe-shi, Hyogo 657-8501, Japan.

* Corresponding author

Abstract

Conventional precast concrete conduits for earth dams are fixed with pre-stressed concrete (PC) steel or bolts at the joints. This leads to problems of ground-following performance and water leakage, which severely hinders the performance of these installations and the wider infrastructure of which they form a part. In this study, a new type of precast concrete conduit without PC steel or bolts is developed. The following three issues are considered in the development of the new conduits: 1) the likelihood of not only bending but also lateral misalignment at the joints between conduits, 2) likelihood of joint separation during earthquakes, especially when the conduit is subjected to axial shaking, and 3) likelihood of leakage under bent and elongated conditions. Each issue is verified through settlement experiments, a shaking-table test, and watertightness tests. Two types

of countermeasure are proposed to suppress lateral misalignment, and new precast concrete conduits with a flexible joint structure and higher watertightness than conventional ones are developed.

Keywords: Earth dams; Model experiment; Precast concrete conduits; Shaking-table test; Watertightness test.

1. Introduction

Piping is one of the most common causes of damage to irrigation earth dams under heavy rainfall conditions, and it has been reported that piping occurs most prominently around conduits (Sherard et al., 1972; Nakajima and Mohri, 1999; Hori et al., 2002; Hori, 2005). One reason for this is the reduction in the horizontal earth pressure due to the concentration of the vertical earth pressure at the top of the conduits (Ngambi et al., 1997). Furthermore, water leakage around the conduits following seismic activity has been reported for two earth dams in Akita Prefecture in Japan, which were damaged by the 1983 Sea of Japan Earthquake (Tani and Hasegawa, 1987).

Detailed surveys have been published on the conduits of earth dams damaged by heavy rainfall and earthquakes, as described above. For in-service earth dams where the damage was not apparent on the surface, Sawada et al. (2021) conducted surveys on the damage (settlement, joint separation, cracks, and leakage) of four concrete conduits of different types (cast-in-place and precast types) and diameters (600–1000 mm). The results showed that cracks were barely visible in the concrete, and the deformation of the conduits was generally absorbed at the joints. In particular, precast concrete

conduits—which have numerous joints per unit length—exhibit a smaller separation per joint than cast-in-place structures, suggesting that the deformation is distributed among several joints. In addition, the deformation of the conduits was not simply distributed according to the overburden pressure; instead, it was strongly affected by the presence of intake structures and cutoff walls, indicating that damage such as joint separations and leakage is common around these structures (Fig. 1). Moreover, leakage traces were recognized in the precast concrete conduits under relatively small joint separations.

As shown in Fig. 2, conventional precast concrete conduits lack flexibility because those featuring rubber seals on both sides are joined with prestressed concrete (PC) bars and bolts. Fujita et al. (2008) conducted horizontal seepage experiments on a conduit with a flexible joint structure (hereinafter referred to as a "flexible structural conduit") under the assumption that the ground beneath the conduit settled locally. The flexible structural conduit was found to follow the local settlement, suppressing the gap development and improving the piping resistance. In the current Japanese design guidelines for small earth dams (Ministry of Agriculture, Forestry and Fisheries, 2015), ductile iron pipes are used as a flexible structural conduit. However, the use of pipes with circular cross-sections makes it difficult to roll and compact the soil at the side of the pipe bottom, which may result in piping through a local decrease in soil density. In addition, the cost of ductile iron pipes is higher than that of concrete conduits.

This study aims to develop a flexible structural precast concrete conduit that is not joined by bolts and PC bars. The lack of such joints may cause the following problems: 1) the increased

likelihood of bending and lateral misalignments at the conduit joints, 2) the increased likelihood of joint separations during earthquakes, particularly when the conduit is subjected to axial shaking, and 3) the increased likelihood of leakage under bent and elongated conditions. Regarding problem (1), a large lateral misalignment reduces the flow cross section and velocity in the conduit. This affects the water flow performance; hence, countermeasures are required if lateral misalignment occurs. Regarding problem (2), the conduit near the intake or outlet (i.e., near the slope) may move significantly during earthquakes because of the low earth pressure and low constraint force; this may produce joint separations and leakage. Regarding problem (3), even if the flexible structure improves the conduit ability to follow the ground deformation, the water storage function of the earth dam is severely hindered when a large leakage occurs in the conduit.

In this study, to examine the three aforementioned problems, the following tests were conducted: 1) settlement tests on a soil container with model conduits within it, designed to investigate the lateral misalignments of the conduit joints, 2) shaking-table tests on a model embankment to investigate the occurrence of joint separation between adjacent conduits, and 3) watertightness tests on full-scale flexible structural precast concrete conduits under elongated and bent conditions for an external water pressure. In this paper, a single conduit is referred to as a “conduit block” (or simply a “block”), and a conduit block connected to another one is referred to as a “conduit.”

2. Lateral Misalignments of Flexible Structural Conduits Subjected to Ground Settlement

Model experiments were conducted to investigate the lateral misalignment of a flexible structural conduit subjected to ground settlement. Twelve conduit blocks were placed in a container with a settling bed; the container bottom was allowed to settle to simulate consolidation settlement and measure the displacement of each conduit block. The lateral misalignment between two conduit blocks was calculated from the displacement results. Experiments on underground structures subjected to compulsory ground deformation (e.g., settlement) have been conducted to investigate the behavior of pipelines subjected to fault displacement (e.g., Ha et al., 2008; Sim et al., 2012; Moradi et al., 2013; Erami et al., 2015) and adjacent to tunnel construction sites (e.g., Marshall et al., 2010), amongst other scenarios. However, no other study has considered the flexible structural conduits evaluated here, except Fujita et al. (2008) mentioned above.

2.1 Experimental Outline of the Settlement Tests on a Soil Container with Model Conduits

The steel soil container (2246 mm × 804 mm × 600 mm) depicted in Figs. 3 and 4 was used for the settlement experiment. As shown in Fig. 3(a) and (b), the bottom of the container was equipped with 22 settlement plates. The conduit block was formed of resin, and its dimensions were 162 and 200 mm in the vertical and axial directions, respectively. These dimensions were approximately 1/7.5 of the full-scale 800 mm-diameter conduit blocks (height: 1200 mm, axial length: 1500 mm) prototyped in Section 4.

In this study, dry silica sand (soil particle density: 2.630 g/cm^3; minimum void ratio: 0.670; maximum void ratio: 1.135) was employed as the soil material, and the mass per unit height was adjusted to achieve a relative density of 40% (dry density: 1.369 g/cm^3). Dry sand was used to improve the ground condition reproducibility in the two experiments. Figure 5 shows the grain size distribution of the silica sand. The sand was uniformly laid to a height of 100 mm above the settlement plate; the conduit blocks were installed thereupon, as shown in Fig. 3(e), and backfilled to a height of 480 mm. Sandbags were positioned on the ground surface in a trapezoidal shape (height: 480 mm; slope: 1:1.5) to simulate an earth dam embankment. Because this study did not consider the deformation of the embankment, the embankment was made of sandbags that were easy to fabricate and offered high reproducibility.

As shown in Fig. 3(c), 12 conduit blocks were installed. Two blocks on either side (i.e., Nos. 1 and 12) half protruded outside the container and were fixed to the container wall to isolate blocks Nos. 2 and 11 from the wall, mitigating the boundary effects and achieving a continuous conduit block. Therefore, the fixings of the blocks at either end did not replicate in-situ conditions (e.g., cutoff walls). As shown in Fig. 3(d), a 4 mm sponge sheet was placed between adjacent blocks to prevent them from contacting each other, and a rubber sheet was used to prevent sand inflow [Fig. 3(e)].

Two cases were tested: one featuring spindle-shaped pins between each conduit block as shown in Fig. 3(d) and the other without such pins. The pins did not resist bending between the blocks but restrained lateral misalignment.

As indicated by the black rectangles in Fig. 6, the settlement experiments were conducted in three stages, labeled Stages 1–3. In Stage 1, the vertical displacement of the central settlement plate was set at –5 mm, and the plates were controlled in such a way that the displacement difference between adjacent plates was approximately equal. When the conduit extension (2246 mm at the inner region of the soil container) was *B,* the settlement (i.e., the absolute value of the maximum vertical displacement) was *S*, and the *S*/*B* ratio was defined as the nondimensional settlement. The *S*/*B* ratio was approximately 2.2×10^{-3} in Stage 1. For Stages 2 and 3, the vertical displacements at the center were set to –10 mm and –20 mm, respectively, and the *S/B* ratios were calculated to be 4.4×10^{-3} and 8.9×10^{-3}, respectively. Similarly, in the field survey results shown in Fig. 1, when the total length of the conduit was 20042 mm (*B*) and the absolute value of the maximum vertical displacement was 30 mm (*S*), $S/B = 1.5 \times 10^{-3}$. That is, although the settlement given in Stage 1 of the model experiment was only 5 mm, its *S*/*B* was approximately 47% larger than that of the field survey.

To measure the vertical displacements of the blocks at each settlement stage, 20 displacement transducers (SDP-100CT, manufactured by Tokyo Measuring Instruments Lab.) were installed on block Nos. 2–11 via wires, as depicted in Figs. 3(a) and 4(a). The wires were encased in aluminum tubes to prevent contact with sand. A displacement transducer (CDP-50, manufactured by Tokyo Measuring Instruments Lab.) was installed on the soil container's exterior because some displacement also occurred in the conduit blocks at both ends.

2.2 Results and Discussion of the Settlement Tests on a Soil Container with Model Conduits

As shown in Fig. 7, the displacement measurements were taken 30 mm from the end of the conduit block in the experiment. The angle θ is expressed as

$$\theta_i = \sin^{-1}\left(\frac{r_i - l_i}{140}\right), \qquad (1)$$

where θ_i is the angle of the i-th block, and l_i and r_i are the vertical displacements measured on the left- and right-hand sides of the i-th block, respectively. The displacement at the end of the block can be obtained using

$$\begin{aligned} L_i &= l_i - 30 \times \sin\theta_i \\ R_i &= r_i + 30 \times \sin\theta_i \end{aligned}, \qquad (2)$$

where L_i and R_i are the left- and right-most displacements of the i-th block, respectively.

Figure 6 depicts the displacements at both ends of the blocks during each settlement stage. The minus sign indicates settlement. Figure 6 shows that, with or without the pin, the conduit blocks settle at the same level as the settling bed displacement, and the blocks follow the ground very well. However, the lateral misalignment between the blocks in the case without pins appears to exceed that observed in the case with pins. Let $\theta_{i\text{-}1\_i}$ and $D_{i\text{-}1\_i}$ be the bending angle and the lateral misalignment between the $(i-1)$-*th* and *i-th* blocks, respectively; it can be calculated using

$$\theta_{i-1\_i} = \theta_i - \theta_{i-1}, \qquad (3)$$

$$D_{i-1\_i} = \left|R_{i-1} - L_i\right|. \qquad (4)$$

Figure 8 depicts the bending angle between the conduit blocks, and Fig. 9 shows the lateral misalignment. In the case without a pin, although the bending angle was small, lateral misalignment

still occurred. By contrast, in the case with pins, the lateral misalignment was suppressed by the simple act of bending. In Stage 1, where the *S/B* (i.e., the ratio of the settlement *S* to the total length of the conduits *B*) was comparatively close to that measured in the field survey, the maximum lateral misalignment was approximately 0.87 mm and 0.33 mm in the cases without and with pins, respectively. The lateral misalignment with pins was suppressed to less than half that of the case without pins. These results suggest that if the blocks are not connected to each other by bolts or PC bars, some lateral misalignments will occur; hence, countermeasures should be taken. In this study, the joint of the conduit block was designed with a spigot and socket joint, allowing it to act as a countermeasure, and a plate was positioned at the bottom of the joint. The effects of these two countermeasures in suppressing lateral misalignment are verified by the shaking tests in Section 3.

3. Verification of Seismic Behavior of Flexible Structural Conduits

Joint separation can occur during earthquakes, especially when the conduit is subjected to axial shaking. A horseshoe-shaped conduit has a larger mass per unit length than a normal circular pipeline. Because the conduit near the slope is subjected to a small earth pressure and is insufficiently restrained, it can move significantly during an earthquake, causing joint separation and leakage. Therefore, the shaking-table tests on a model embankment (height: 1.25 m) were conducted to verify whether joint separation occurred between adjacent conduits. Several previous studies have performed shaking-table tests for

earth dams (e.g., Torisu et al., 2010; Sawada et al., 2018; Sawada et al., 2019); however, no study has done so for embankments including conduits.

3.1 Experimental Overview of the Shaking-Table Tests on a Model Embankment

In this experiment, a steel soil container (5.5 m × 2.0 m × 3.0 m) was installed on a 6 m long and 4 m wide shaking-table (owned by the National Agriculture and Food Research Organization), and an earth dam embankment model was constructed inside the container, as shown in Figs. 10 and 11. The model conduit had a diameter of 200 mm, a height of 300 mm, and an axial length of 375 mm. This is a quarter of the size of the 800 mm-diameter precast concrete conduits (height: 1200 mm; axial length: 1500 mm) fabricated in Section 4. To determine the density of the conduit block, the relation between the inertial force that affects the joint separation and the resistance (frictional) force that suppresses it is discussed based on the similarity law. The inertial force F is expressed as

$$F = m \cdot \alpha = \left(\rho V\right) \cdot \left(K_h g\right), \qquad (5)$$

where m is the mass of the conduit block; α is the horizontal acceleration; ρ and V denote the density and volume of the conduit block, respectively; K_h is the horizontal seismic intensity; and g is the acceleration due to gravity. The resistance force R is the frictional force acting around the conduit block; it is expressed as

$$R = A \cdot p \cdot \mu, \qquad (6)$$

where A is the surface area of the conduit block in contact with the soil, p is the normal earth pressure acting on the conduit block surface, and μ is the friction coefficient between the block and soil. The ratio F/R must be identical for the prototype and model (scale: $1/N$). Because K_h and g are assumed identical between the prototype and model, the following equation can be obtained

$$\frac{F_p}{R_p} = \frac{\rho_p V_p K_{h\_p} g_p}{A_p p_p \mu_p} = \frac{\rho_m \left(N^3 V_m\right) K_{h\_m} g_m}{\left(N^2 A_m\right)\left(N p_m\right)\mu_m} = \frac{\rho_m V_m K_{h\_m} g_m}{A_m p_m \mu_m} = \frac{F_m}{R_m}. \qquad (7)$$

Here, the subscripts p and m denote the prototype and model, respectively. To satisfy Eq. (7), the density ρ and friction coefficient μ should be the same for the prototype and the model. Therefore, the conduit blocks in this experiment were constructed of high-strength mortar, and the density of the conduit blocks was adjusted to match that of the real concrete. It is assumed that there is no significant difference in the coefficients of friction between the mortar and the concrete. From the above discussion, it can be concluded that these model conduit blocks satisfy the similarity law for the main purpose of this study, which is to examine the joint-separation behavior of precast concrete conduits and the resistance force (frictional force) that suppresses them.

From the results of the settlement experiments in Section 2, the conduit developed here was selected as having a 25 mm-axial-long spigot and socket joint to suppress the lateral misalignment; furthermore, a plate (thickness: 25 mm; conduit axial length: 100 mm) was installed beneath the conduits. A total of 10 conduits were installed (spaced 1 mm apart), and a sponge packing was attached to the spigot side to maintain spacing. Rubber was installed at the actual joint to prevent water inflow. It provides a small amount of resistance to the joint separation. If the rubber is reproduced in the model

experiment, this resistance may become excessive, and the separation may be underestimated. Therefore, watertight rubber was not installed at the model joints. As shown in Fig. 11, a pile simulating a cutoff wall was installed at the bottom of the second conduit block on the right-hand side. This reproduced the suppressive effect of the cutoff wall on the conduit settlement, as shown in the damage survey depicted in Fig. 1.

An earth dam embankment model (height: 1.25 m, crest width: 0.75 m, slope gradient: 1:1.5) was constructed on a 1-m-high base. This experiment focuses upon the seismic behavior of the conduit rather than the deformation of the earth dam embankment. When the embankment was subjected to seismic-motion-induced sliding failure, the earth pressure acting on the conduit changed significantly; the restraining force also varied. Although such cases may occur in practice, the purpose of this study was to clarify the effect of restraining force differences on the conduit behavior. In this experiment, the embankment was reinforced with three layers of polyethylene reinforcement to protect the embankment from seismic-motion-induced sliding failure. Kasumigaura sand (soil particle density: 2.719 g/cm^3, maximum dry density: 1.510 g/cm^3, optimum water content, 21.2%) was employed as the ground material, and the degree of compaction on the base and embankment was set at 85%. Although 85% compaction is much lower than the 95% specified in the earth dam design guidelines (Ministry of Agriculture, Forestry and Fisheries, 2015), reproduction of the conduit block displacement and the joint separation at the fixed part (cutoff wall) were attempted by intentionally causing the base to settle. Figure 5 shows the grain size distribution of the Kasumigaura sand.

Sinusoidal waves of 5 Hz (period: 0.2 s) with amplitudes of 50, 200, 300, and 400 gal were applied for 12 s, including a 2 s taper part. Here, the relationship between the model and prototype time is expressed as

$$T_p = \sqrt{\frac{L_p}{g_p}} = \sqrt{\frac{NL_m}{g_m}} = \sqrt{N}T_m . \qquad (8)$$

Therefore, the 0.2 s shaking period in the 1/4-scale model experiment (N = 4) equates to 0.4 s in real terms, which is relatively close to the dominant period of the earth dam embankment, according to the constant microtremor records measured by Saito et al. (2007). The acceleration of the shaking-table under 400 gal shaking is shown in Fig. 12 as an example.

To investigate joint separations, two displacement transducers (CDP-50; manufactured by Tokyo Measuring Instruments Lab.) were installed in each conduit block (four displacement transducers on each side of conduit blocks Nos. 2, 6, 9, and 10) for a total of 26 units. To measure the settlement of the conduit blocks, 12 displacement transducers (SDP-100CT; manufactured by Tokyo Measuring Instruments Lab.) were installed at the tops of the blocks via wires. As described for the settlement experiment, the wires were protected by aluminum pipes to prevent them from contacting the soil. In addition, accelerometers were installed inside conduit block Nos. 2, 6, and 9 and in the soil surrounding these blocks to examine the phase differences between the surrounding soil and conduit blocks.

3.2 Results and Discussion of the Shaking-Table Tests on a Model Embankment

A) Verification of inertial-force-induced joint separations between conduit blocks

Figure 13 shows the time variation of the relative axial displacements between conduit blocks No. 1 and No. 2, No. 5 and No. 6, and No. 9 and No. 10 during 400 gal shaking. Figure 13 indicates that the displacements vary with respect to vibration. The displacement generated between conduit blocks by the inertial force was seen to correspond to the vibration component, taking into account the dependence of the inertial force on acceleration. The displacements (excluding the vibration component) were attributed to the ground deformation. Here, the displacement produced by the inertial force (vibration component) was extracted using the method shown in Fig. 14. The original time-series data shown in Fig. 14(a) were subjected to a smoothing process with a cutoff frequency of 5 Hz, which corresponds to the shaking frequency [Fig. 14(b)]. Then, the vibration component was extracted by subtracting the smoothed displacement from the original displacement data [Fig. 14(c)]. The maximum amplitude of the vibration component is defined as the maximum inertial-force-induced displacement. Figure 15 shows the distribution of this maximum displacement. As seen in Fig. 15, the maximum displacement, as measured by the displacement transducers installed on the upper sides of the conduit blocks, tended to be smaller at the center and larger toward the edges. This indicates that at the center (where the overburden pressure is high), the restraining force acting on the conduit block is large and the inertial-force-induced displacement is small. Meanwhile, the restraining force is small and the displacement is relatively large at the edges. At the bottom of the conduit blocks, a displacement of approximately 3 mm was observed 1500 mm from the center (between block Nos. 9 and 10). This may be due to the influence of fixed piles, although the exact cause is unknown. However, judging from the insertion length of the joint (24 mm), the maximum displacement (3 mm) does not appear to cause leakage. Therefore, the displacement due to the inertial force of the conduit block is not a major problem against the large shaking of 400 gal, even at the end where the restraining force is small. Figure 16 shows the acceleration records of the soil and conduit blocks during the 400 gal shaking. The accelerations of the conduit block and the surrounding soil were almost overlapping, and no phase

difference was observed among them. This indicates that the conduit blocks move in unison with the surrounding soil, and the soil provides an effective restraining force.

B) Verification of the effects of lateral-misalignment-suppressing countermeasures

To suppress the lateral misalignment between the conduit blocks, a 25 mm-axial-length spigot and socket joint was employed, and a plate (thickness: 25 mm, conduit axial length: 100 mm) was installed beneath the conduits. To verify these effects, the vertical displacements of the conduit blocks were measured, and the lateral misalignment was verified. In particular, the displacement of the fixed component and the conduit blocks on both sides were considered to be large, and as depicted in Fig. 11, numerous displacement gauges were installed there. However, as shown in Fig. 17, the aluminum pipe protecting the wire running between the displacement transducer and conduit block was tilted, and the vertical displacement could not be measured accurately. Instead of measuring the vertical displacement, the soil was carefully removed from the embankment after 400 gal of shaking, and the conduit blocks were visually inspected (Fig. 17). A large lateral misalignment was identified between fixed component No. 9 and the adjacent conduit block No. 8. However, no other misalignment was observed, suggesting that the two countermeasures installed between the conduit blocks were effective.

Table 1 shows the settlement S and nondimensional settlement S/B measured by the displacement transducer installed at the top of the conduit block. The settlement was taken as the average of the absolute vertical displacement values near the center of conduit blocks Nos. 5 and 6. The nondimensional settlement was calculated by dividing the settlement by the total length of the conduit (3758 mm). From this table, the nondimensional settlement after 400 gal shaking can be

identified as $S/B = 2.0 \times 10^{-2}$, which is more than 13 times larger than the value of $S/B = 1.5 \times 10^{-3}$ obtained in the field survey (Fig. 1); hence, the level of settlement appears unrealistic. Therefore, displacement between blocks No. 8 and No. 9 is unlikely to develop. However, it is desirable to install more flexible structural conduit blocks at fixed points (e.g., near the cutoff wall); judging from the results of past damage investigations by Sawada et al (2021), large local deformations can occur there (e.g., Fig. 1).

4. Watertightness Verification of Flexible Structural Conduit under Bent and Elongated Conditions

Even if the conduit has a flexible structure and can follow the ground deformation, a large leakage at the joints of the conduit will severely limit the water-storage performance of the earth dam. Therefore, watertightness tests were conducted by applying an external water pressure (equivalent to the water level of the earth dam under bent and elongated conditions) between the conduit blocks. An 800 mm-diameter precast concrete conduit was produced as the test specimen, taking into account the findings in Sections 2 and 3.

4.1 Methodology of the Watertightness Tests on Full-Scale Precast Flexible Structural Conduits

The flexible structural precast concrete conduit block constructed in this study had an 800 mm-diameter, with a height, bottom width, and axial length of 1200, 1254, and 1500 mm, respectively, as shown in Fig. 18. The axial length of the spigot and socket joint was 100 mm, and earthquake-resistant rubber rings were installed. The rubber ring was developed by the authors. The material of the flexible rubber parts is EPDM (Ethylene Propylene Diene Monomer) rubber. The configuration shown in Fig. 18 (a) is the standard flexible structural precast concrete conduit developed in this study. Alongside the standard type, a new type of conduit block (hereafter referred to as the "highly flexible structure type") was developed to realize an even more flexible structure by installing an earthquake-resistant flexible rubber at the center of the conduit block. In the test, the connecting components of the conduit blocks or the spaces between the rubber components were covered with rubber, and water pressure was applied to the space to check for leakage on the conduit inner surface (Fig. 19).

The test conditions are presented in Table 2. The test was performed under normal installation conditions with a joint spacing of 5 mm for the standard type and 20 mm for the highly flexible structure type. For the elongation conditions, the joint spacing was set as 35 mm (standard type) and 70 mm (highly flexible type). Furthermore, for the bending conditions, the joint spacing was set as 10 mm on the upper side and 40 mm on the lower side (bending angle: 1.4°) for the standard type and 20 mm on the upper side and 70 mm on the lower side (bending angle: 2.3°) for the highly flexible structure type. For each test condition, a specified external water pressure was applied and maintained for 3 min to check for leakage from the joints. The duration (3 min) was determined according to the

Japanese Standard for precast concrete products (Japanese Industrial Standard, 2016) and for reinforced concrete box culverts for sewerage (Japan Sewage Works Association, 2012). The maximum test water pressure was set as 0.15 MPa because the earth dam had a height of 15 m or less.

4.2 Results and Discussion of the Watertightness Tests on Full-Scale Precast Flexible Structural Conduits

No leakage was observed in the results for all test conditions. Therefore, the separation and bending angle (which were set as the test conditions) are given as the permitted (or guaranteed) values of the proposed precast concrete conduit under a water pressure of 0.15 MPa, which should be considered in the design. The specific design method is not discussed here; however, one method involves calculating the expected settlement from in-situ tests and numerical analysis then planning the arrangement of the conduit blocks. Next, the separation and bending angle can be determined under the assumption that lateral misalignment does not occur. It is sufficient to confirm that these values are within the values obtained when considering the safety factor for the permitted separations and bending angles described above.

5. Summary and Conclusion

In this study, to develop a flexible structural precast concrete conduit that can follow ground deformation, the PC bars and bolts, which are conventionally installed at the joints between the conduit

blocks, were removed. Three possible problems were experimentally evaluated, and the findings are summarized as follows:

1) When the PC bars and bolts are removed from the conduit block joints, both bending and lateral misalignment can occur simultaneously, decreasing the water flow performance. The lateral misalignment of the conduit blocks was investigated by settling the bottom of the soil container. The results show that lateral misalignment occurs when the conduit blocks are not connected via PC bars and bolts. In this study, two countermeasures were proposed to reduce the lateral misalignment between the conduit blocks: the use of a spigot and socket joint and a plate installed beneath the conduit interfaces. Subsequent shaking-table tests showed that the lateral misalignment was suppressed, and the effectiveness of the countermeasures was verified.

2) When the PC bars and bolts are removed from the conduit block joints, the joints can separate during earthquakes, particularly when the conduits are subjected to longitudinal shaking. A shaking-table test was performed on a 1.25-m-high model embankment to verify whether joint separation occurred between adjacent conduits. The resulting displacement at the end of the conduit was relatively large due to the low overburden pressure. However, judging from the insertion length of the joint, the displacement was not large enough to cause leakage, and the inertial-force-induced displacement was not a major problem.

3) When the PC bars and bolts are removed from the conduit block joints, the structure is expected to become more flexible; however, leakage under the elongated and bent conditions should be considered. Watertightness tests were conducted on 800-mm-diameter precast concrete conduit blocks in the elongated and bent conditions under external water pressure. A prototype conduit block with an earthquake-resistant rubber ring on the spigot side of the joint was developed. To realize a more flexible structure, a highly flexible structure conduit block prototype with an earthquake-resistant flexible rubber in its center was developed. The joints and flexible rubber parts were subjected to water pressures equivalent to the maximum water depth (15 m) predicted for an earth dam under the specified elongated and bent conditions; water leakage did not occur in either case.

In summary, two countermeasures were proposed, and their effectiveness at addressing the three problems associated with the removal of the PC bars or bolts from the joints of conventional precast concrete conduits were verified. A new precast concrete conduit with improved ground-following performance was also developed. In future, it will be essential to study the design method and construction challenges of this flexible-structure precast concrete conduit to further enhance the robustness and durability of earth dams.

Data availability

Some or all data, models, or code that support the findings of this study are available from the corresponding author upon reasonable request.

Acknowledgement

This work was conducted through a public–private partnership research and development project for new technology in Japan's Ministry of Agriculture, Forestry, and Fisheries.

References

Erami, M. H., Miyajima, M., Kaneko, S., Toshima, T., Kishi, S. 2015. "Pipe–soil interaction for segmented buried pipelines subjected to dip faults." *Earthq. Eng. Struct. Dyn.*, 44(3), 404-417. https://doi.org/10.1002/eqe.2476.

Fujita, N., Mohri, Y., and Tanaka, R. 2008. "Seepage flow along outlet conduit in reservoir embankment: restraint of piping failure with flexible conduit." *Transactions of The Japanese Society of Irrigation, Drainage and Rural Engineering*, 255, 57–68.

Ha, D., Abdoun, T. H., O'Rourke, M. J., Symans, M. D., O'Rourle, T. D., Palmer, M. C., Stewart, H. E. 2008. "Centrifuge modeling of earthquake effects on buried high-density polyethylene (HDPE) pipelines crossing fault zones." *J. Geotech. Geoenviron. Eng.*, 134(10), 1501–1515. https://doi.org/10.1061/(ASCE)1090-0241(2008)134:10(1501).

Hori T. 2005. "Damages of small earth dams for irrigation induced by heavy rainfall." *Bulletin of the National Research Institute of Agricultural Engineering*, 44, 139–247.

Hori T., Mohri Y., Aoyama S. 2002 "Causes and features of damage to small earth dams induced by heavy rainfall." *Transactions of the Japanese Society of Irrigation, Drainage and Reclamation Engineering*, 218, 127–137.

Japanese Industrial Standard. 2016 "JIS A 5363 Precast concrete products - General rules for methods of performance test." (in Japanese).

Japan Sewage Works Association. 2012 "JSWAS A-12 Reinforced concrete box culvert for Sewerage (Nominal Dimension 600×600-3500×2500)." (in Japanese).

Marshall, A. M., Klar, A., Mair, R. J. 2010. "Tunneling beneath buried pipes: view of soil strain and its effect on pipeline behavior." *J. Geotech. Geoenviron. Eng.*, 136(12), 1664–1672. https://doi.org/10.1061/(ASCE)GT.1943-5606.0000390.

Moradi, M., Rojhani, M., Galandarzadeh, A., Takada, S. 2013. “Centrifuge modeling of buried continuous pipelines subjected to normal faulting.” *Earthq. Eng. Eng. Vib.*, 12(1), 155–164. https://doi.org/10.1007/s11803-013-0159-z.

Ministry of Agriculture, Forestry and Fisheries (2015): Design guideline of land improvement project “Small earth dam”

Nakashima, M., Mohri, Y. 1999. “Consideration of the design for outlet works of small earth dam against fatal accidents.” *Technical report of the National Research Institute of Agricultural Engineering*, 197, 73–81.

Ngambi, S., Nakano, R., Shimizu, H., Nishimura, S. 1997. “Cause of leakage along the outlet conduit underneath a low fill dam with special reference to hydraulic fracturing.” *Transactions of The Japanese Society of Irrigation, Drainage and Reclamation Engineering*, 188, 93–102. https://doi.org/10.11408/jsidre1965.1997.263.

Saito, A., Hasegawa, S., Yamanaka, M., Kagawa, Y., Hayashi, K. 2007. “Evaluation of motion amplification of small earth dam by surface wave survey and microtremor measurement.” *Proceeding of the JSCE Earthquake Engineering Symposium*, 29, 713–721. https://doi.org/10.11532/proee2005a.29.713.

Sawada, Y., Arita, J., Omori, M., Kawabata, T. 2021. “Damage characteristics of conduits in irrigation earth dams.” *Paddy and Water Environ.*, 19(1), 239–247. https://doi.org/10.1007/s10333-020-00835-2.

Sawada, Y., Nakazawa, H., Oda, T., Kobayashi, S., Shibuya, S., and Kawabata, T. 2018. “Seismic performance of small earth dams with sloping core zones and geosynthetic clay liners using full-scale shaking table tests.” *Soils Found.*, 58(3), 519–533. https://doi.org/10.1016/j.sandf.2018.01.003.

Sawada, Y., Nakazawa, H., Take, W. A., and Kawabata, T. 2019. “Effect of installation geometry on dynamic stability of small earth dams retrofitted with a geosynthetic clay liner.” *Soils Found.*, 59(6), 1830–1844. https://doi.org/10.1016/j.sandf.2019.08.007.

Sherard, J. L., Decker, R. S., and Ryker, N. L. 1972. “Hydraulic fracturing in low dams of dispersive clay.” *Proc. of the Specialty Conference on Earth and Earth-Supported Structures*, 653–689.

Sim, W. W., Towhata, I., Yamada, S., Moinet, G. J. M. 2012. “Shaking table tests modelling small diameter pipes crossing a vertical fault.” *Soil Dyn. Earthq. Eng.*, 35, 59–71. https://doi.org/10.1016/j.soildyn.2011.11.005.

Tani, S., Hasegawa, T. 1987. “Earthquake damage on earth dam by the 1983 Nipponkai-Chubu Earthquake.” *Journal of Japanese Society of Agriculture Engineering*, 55(10), 17–25.

Torisu, S. S, Sato, J., Towhata, I., Honda, T. 2010. “1-G model tests and hollow cylindrical torsional shear experiments on seismic residual displacements of fill dams from the viewpoint of seismic performance-based design.” *Soil Dyn. Earthq. Eng.*, 30(6), 423–437.

1

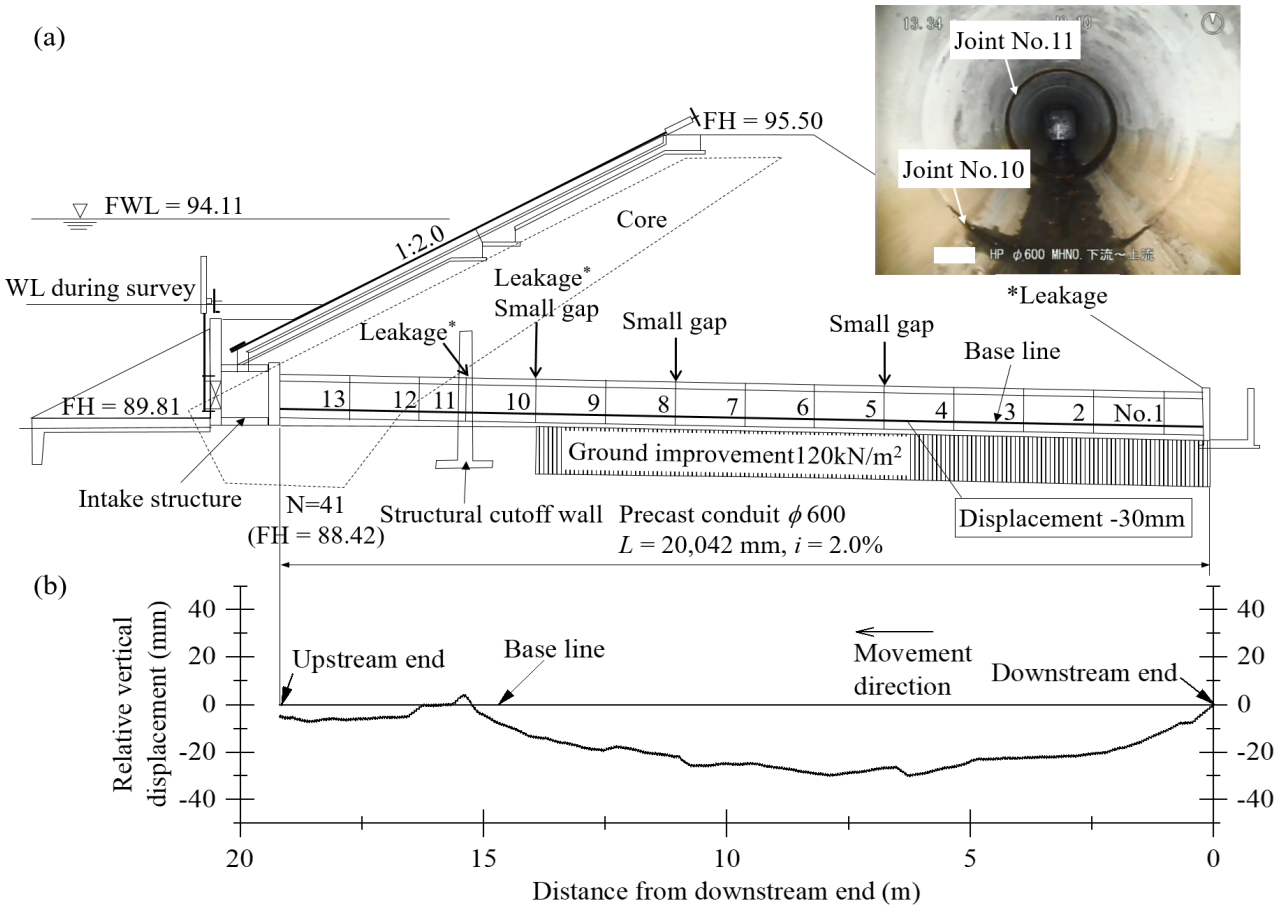

Fig. 1. Damage survey results in a precast concrete conduit: a) damage conditions (i.e., the emergence of leakage and joint separations) and b) relative vertical displacement (Sawada et al., 2021).

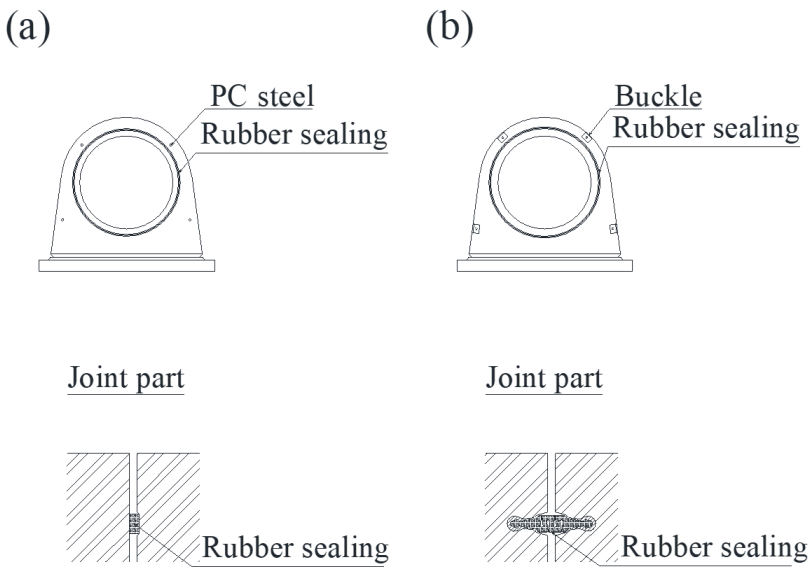

Fig. 2. Cross-section of conventional nonflexible precast concrete conduit: a) PC steel and b) bolt fixings (Sawada et al., 2021).

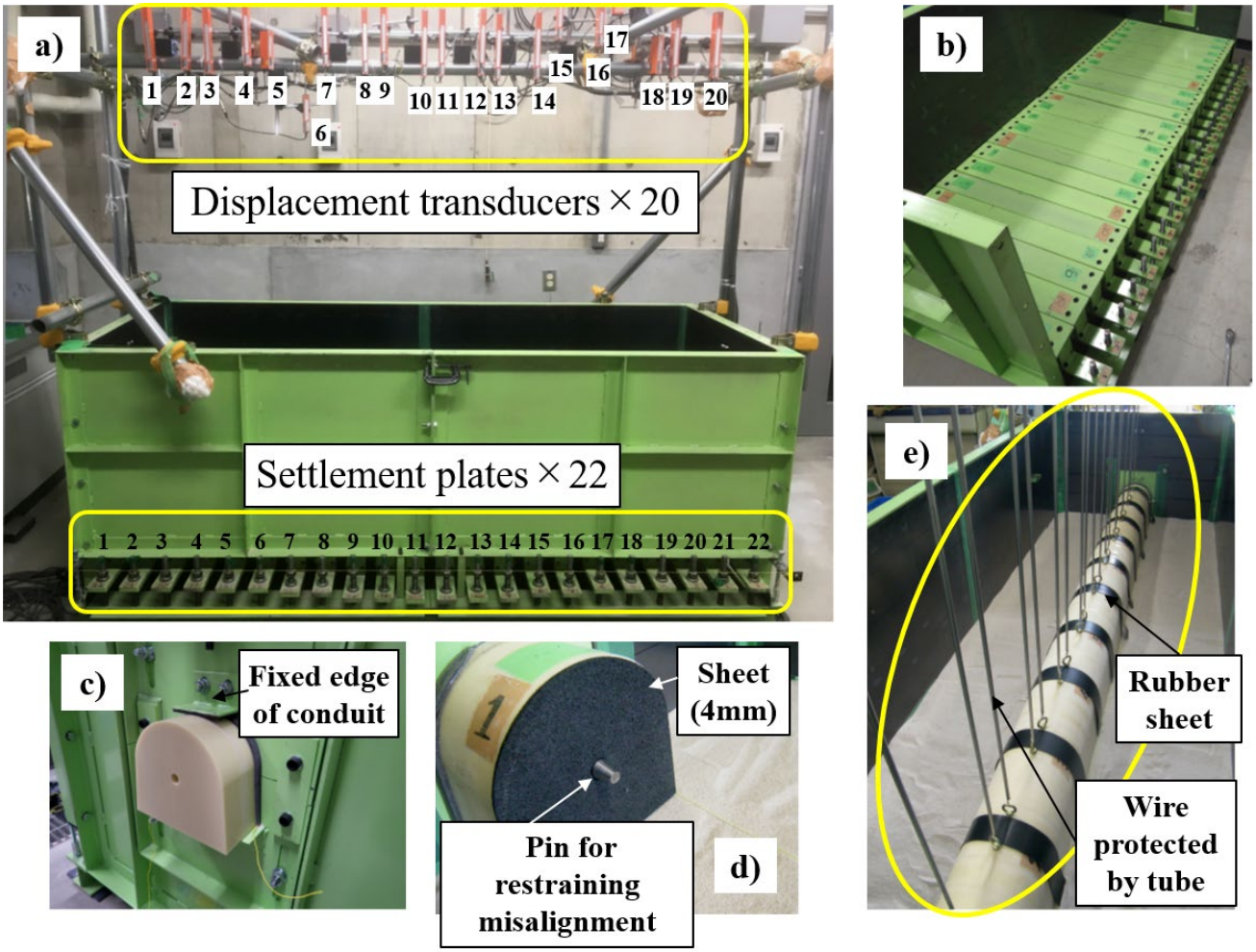

Fig. 3. Equipment for settlement experiment: a) soil container, b) settlement plates beneath the soil container, c) fixed edge of conduit, d) pin for restraining misalignment, and e) conduit blocks.

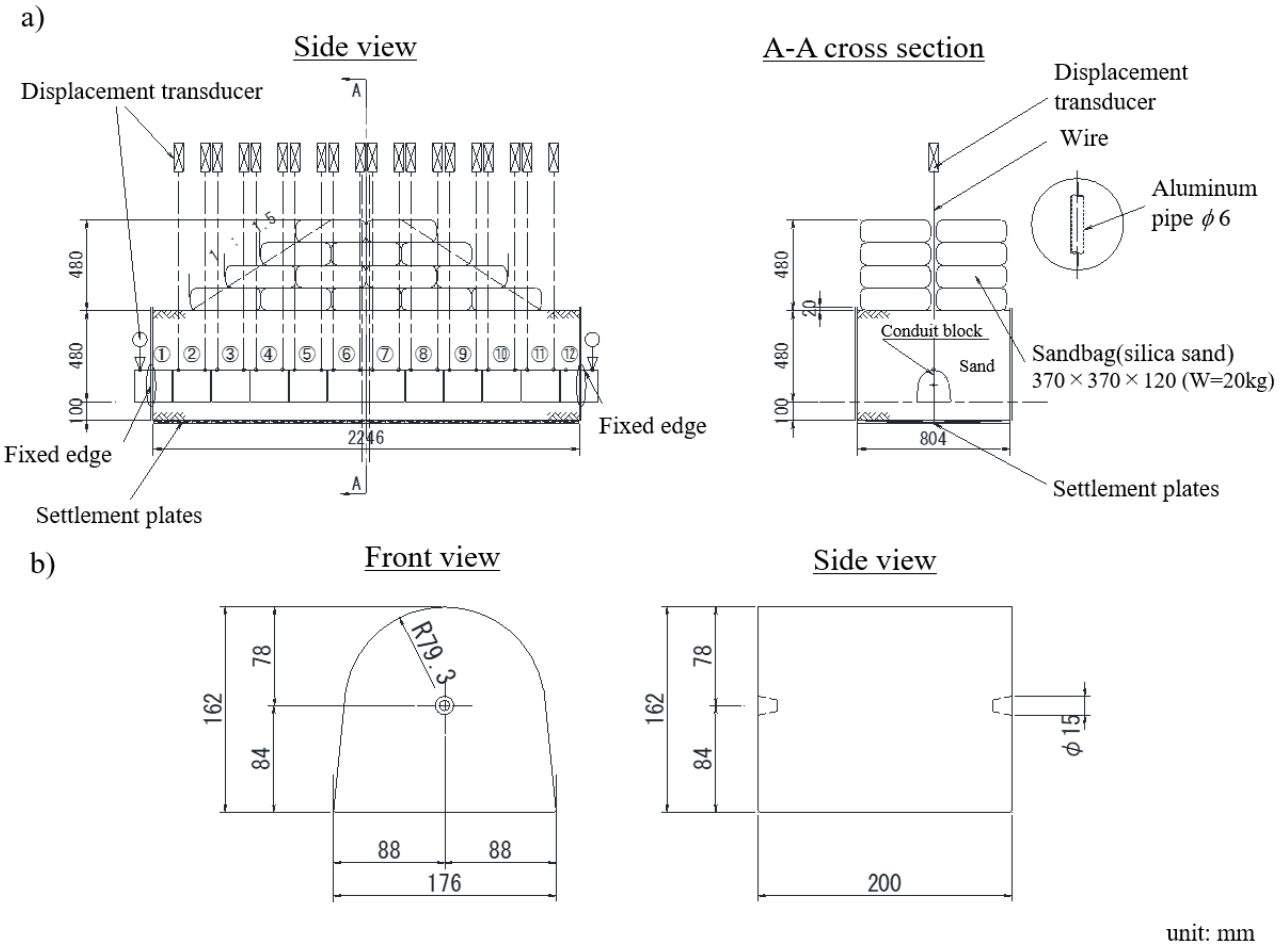

Fig. 4. Settlement experiment setup: a) side view and cross section of the experiment and b) front and side views of the conduit block.

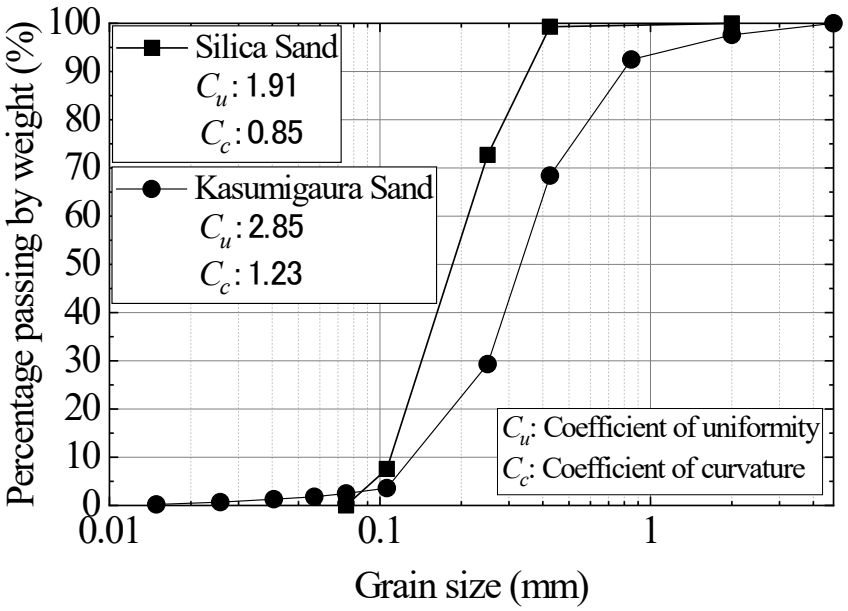

Fig. 5. Grain-size distributions of soils used in this study (silica sand for the settlement experiment and Kasumigaura sand for the shaking-table test).

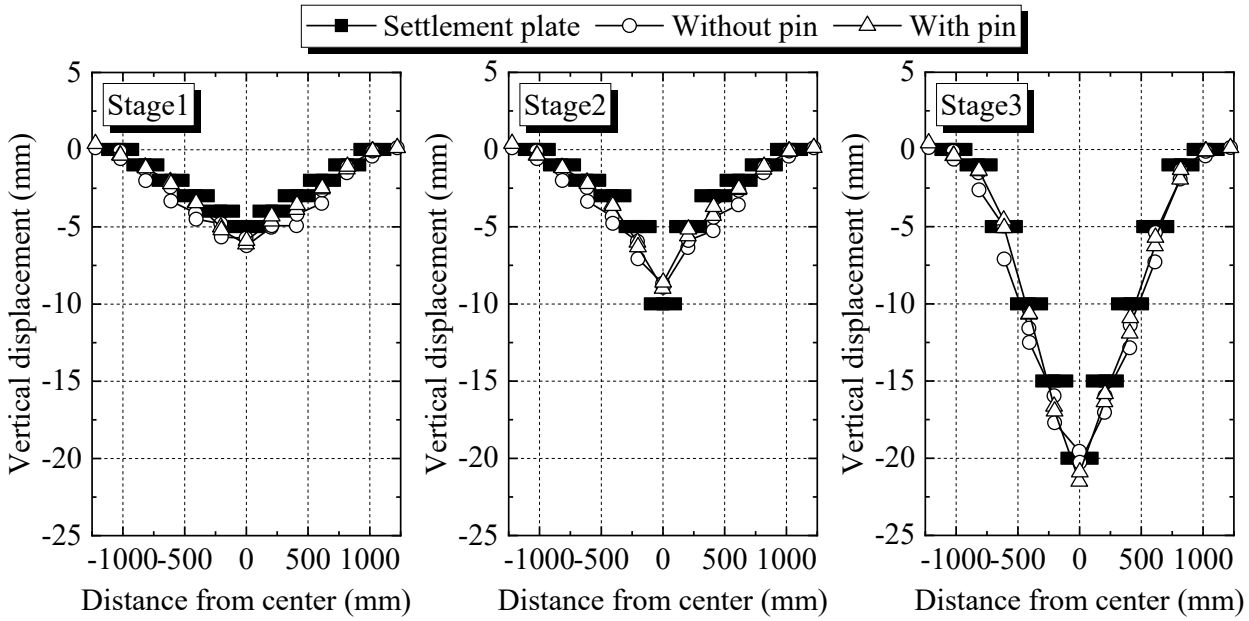

Fig. 6. Vertical displacement of settlement plate and conduit blocks.

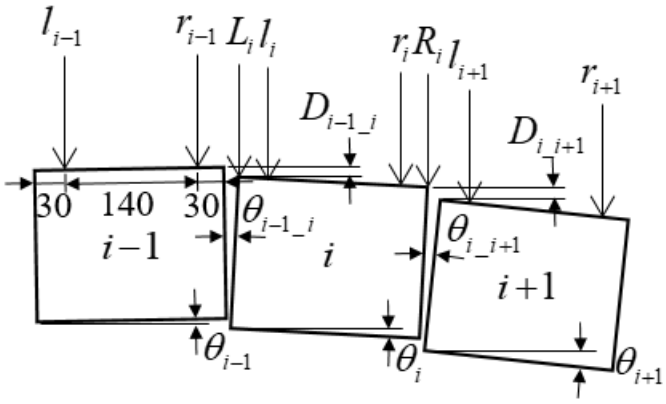

Fig. 7. Bending angle and lateral misalignment between conduit blocks.

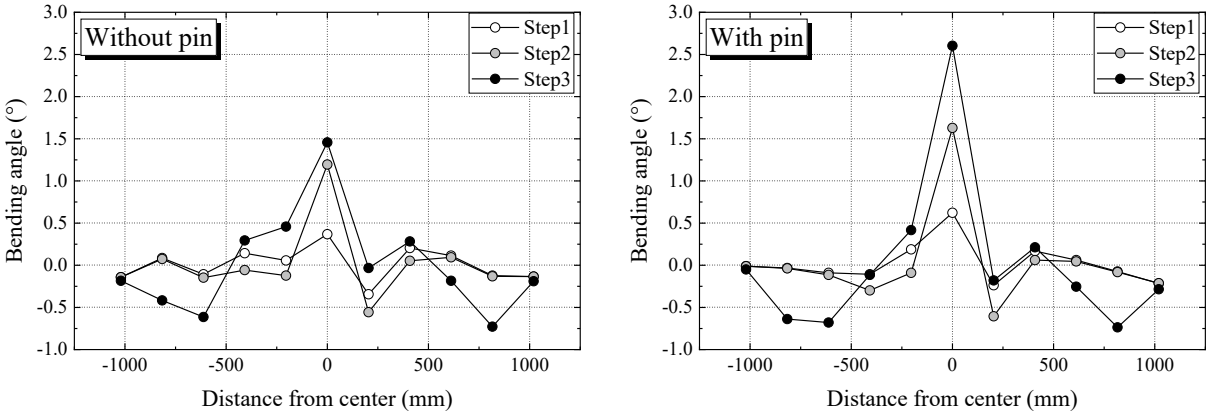

Fig. 8. Bending angle between conduit blocks.

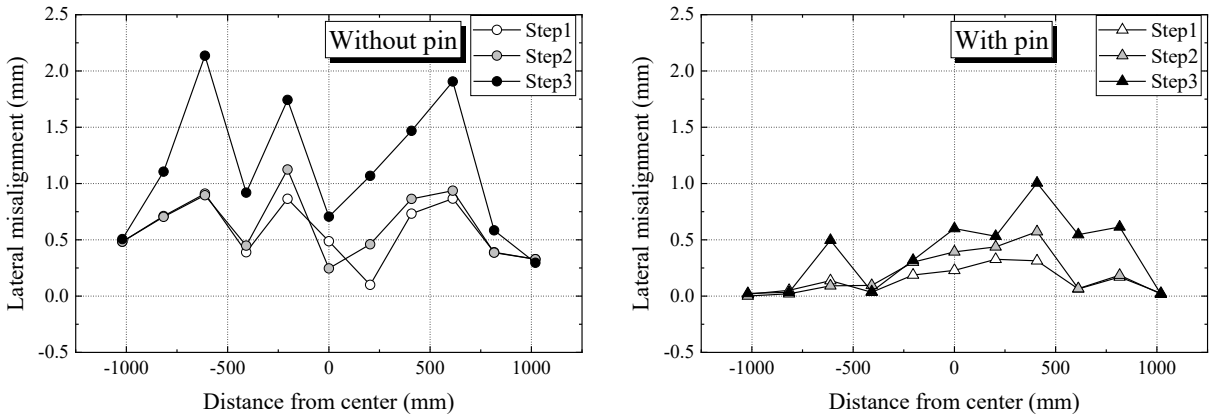

Fig. 9. Lateral misalignment between conduit blocks.

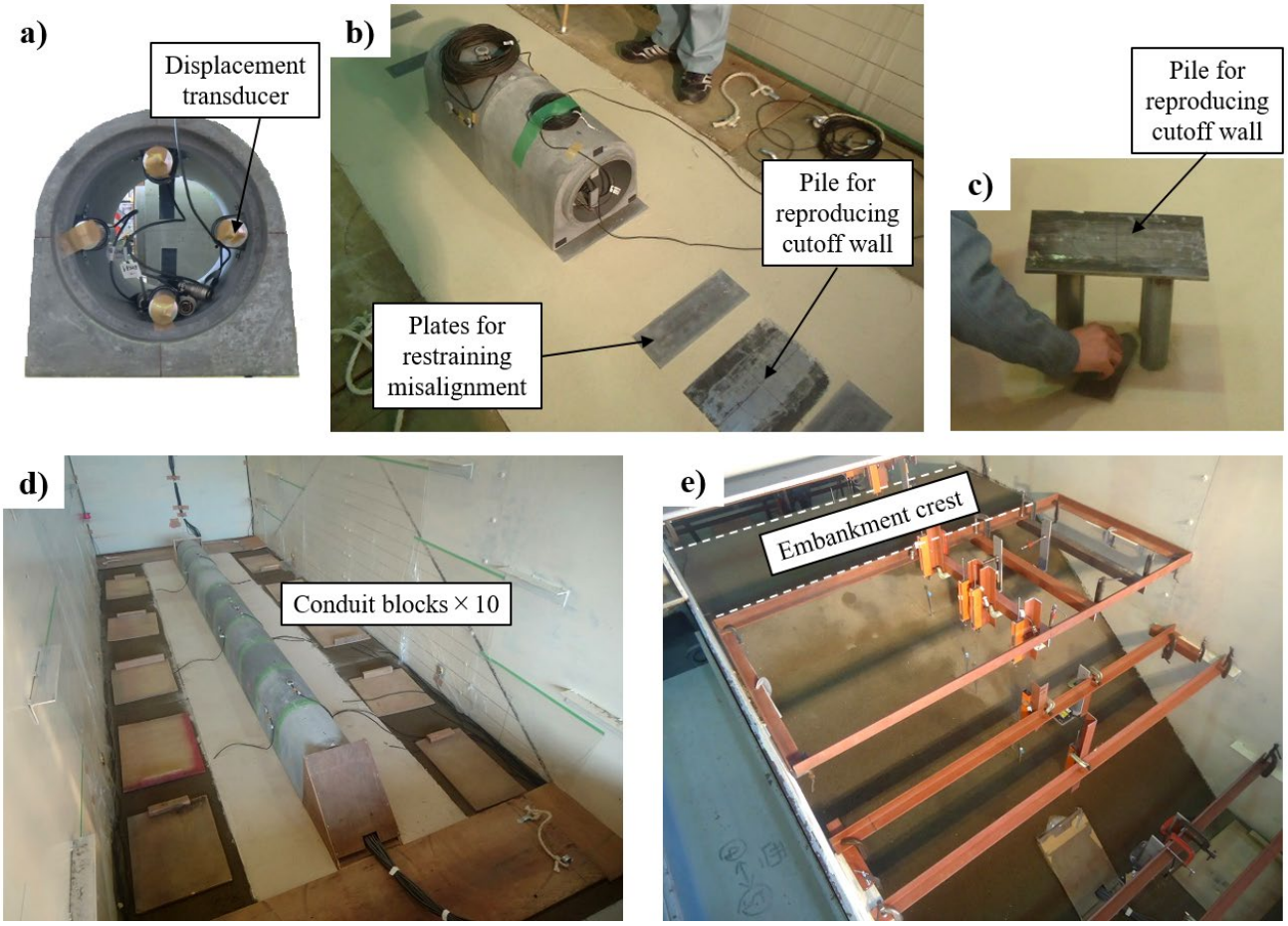

Fig. 10. Shaking-table test equipment: a) conduit block model, b) plate for restraining misalignment, c) pile for reproducing cutoff wall, d) conduit block setup, and e) embankment model.

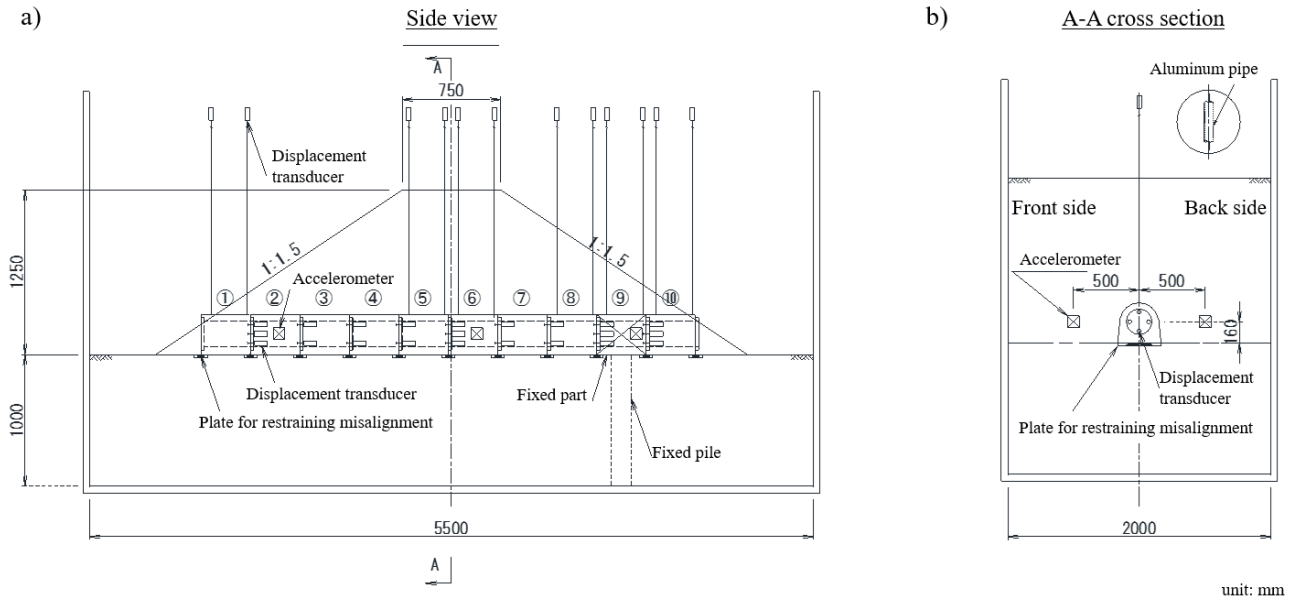

Fig. 11. Shaking-table test setup: a) side view and b) cross-section.

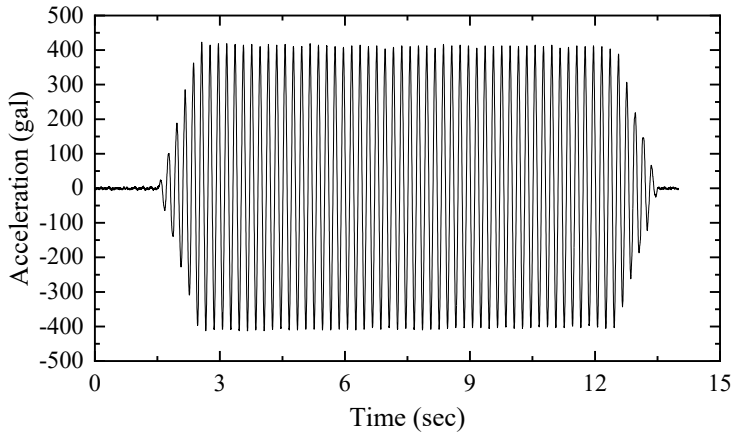

Fig. 12. Acceleration of shaking-table (400 gal).

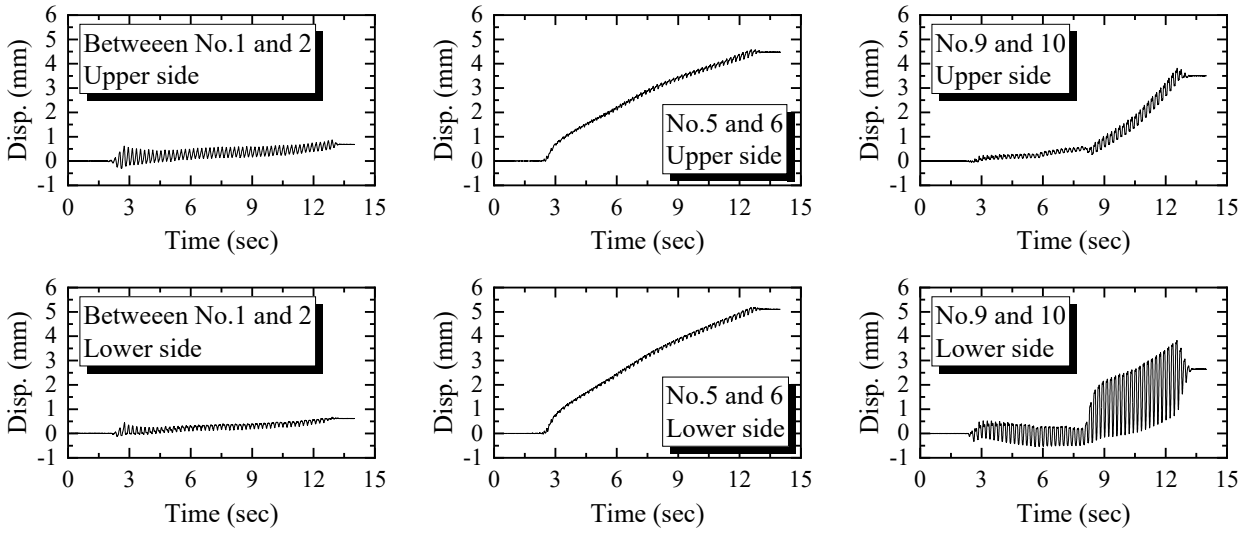

Fig. 13. Axial displacement of conduit block joints (400 gal).

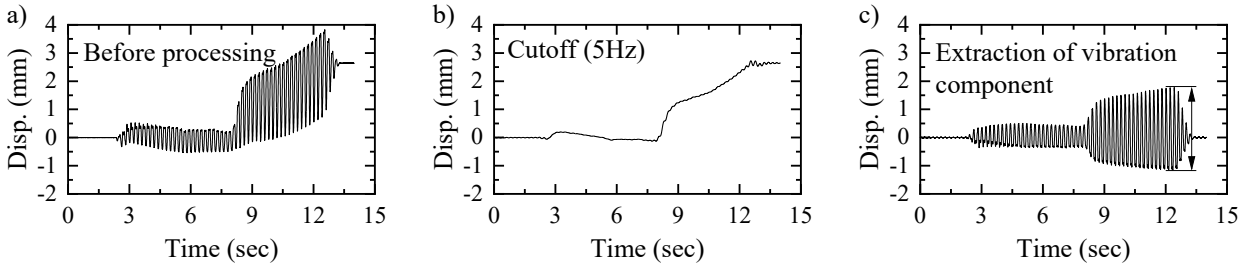

Fig. 14. Vibration component extraction: a) original displacement time series, b) post-cutoff process at 5 Hz, and c) extracted vibration components.

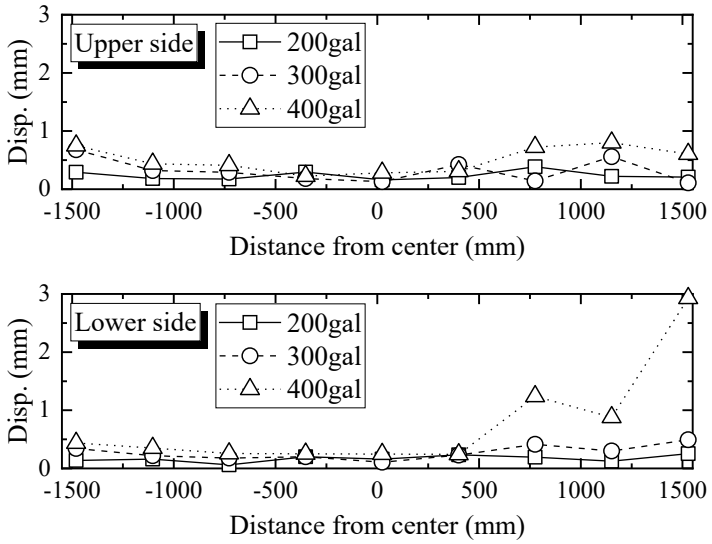

Fig. 15. Maximum axial displacement of conduit block joints.

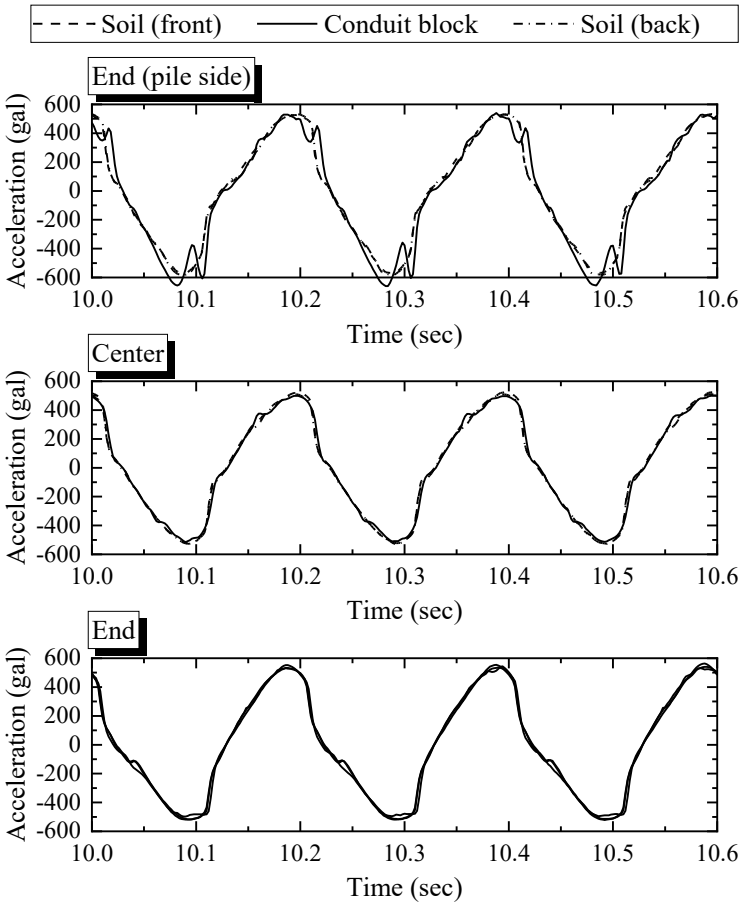

Fig. 16. Recorded acceleration of soils and conduit blocks.

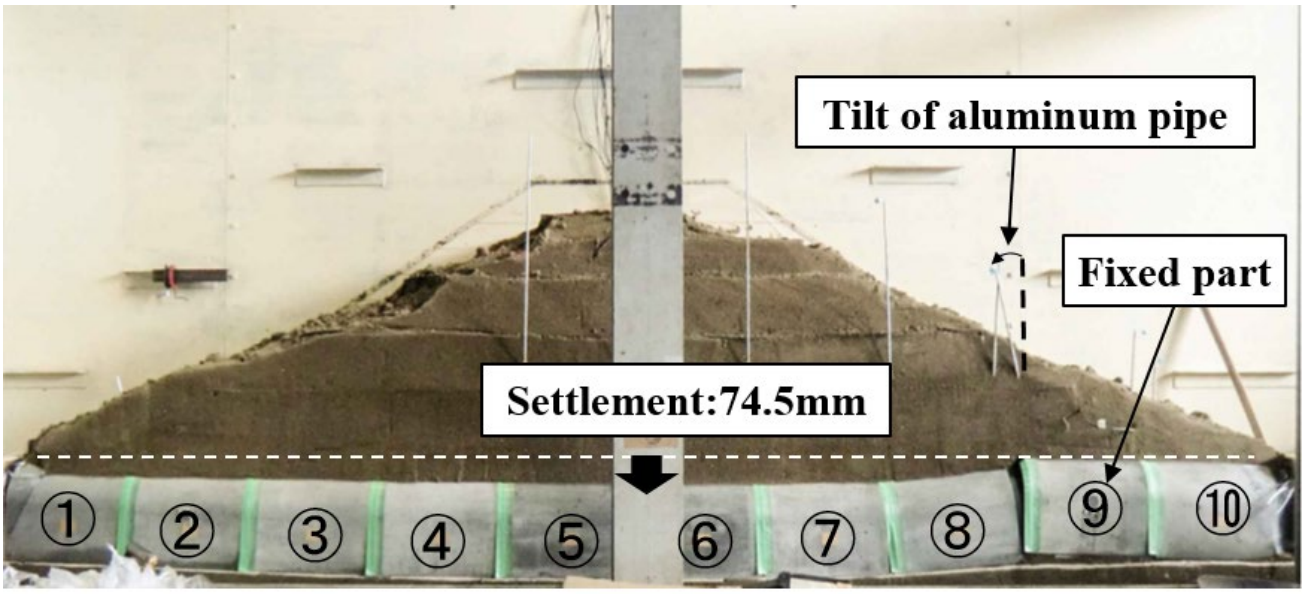

Fig. 17. Conduit blocks excavated after the shaking-table test.

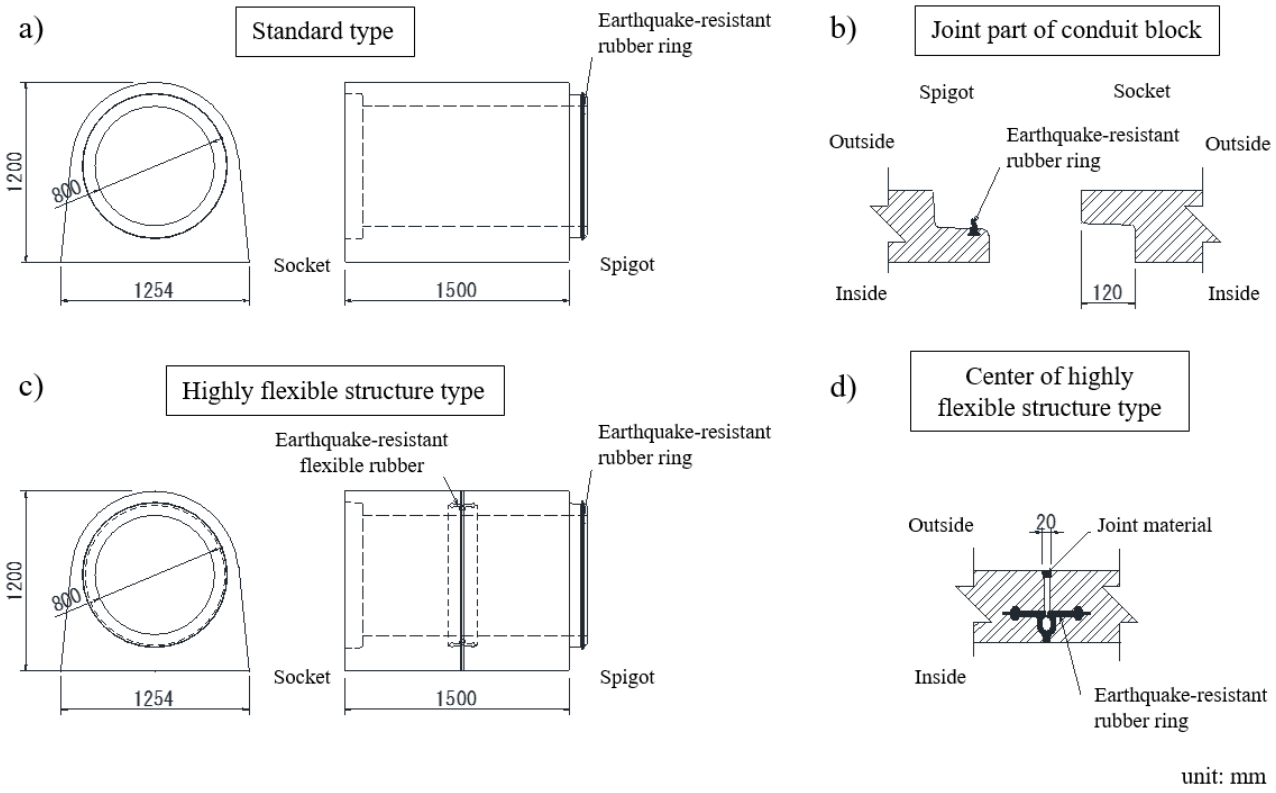

Fig. 18. Prototype conduit blocks for watertightness tests: a) standard type, b) conduit block joint, c) highly flexible structure type, and d) center of highly flexible structural type.

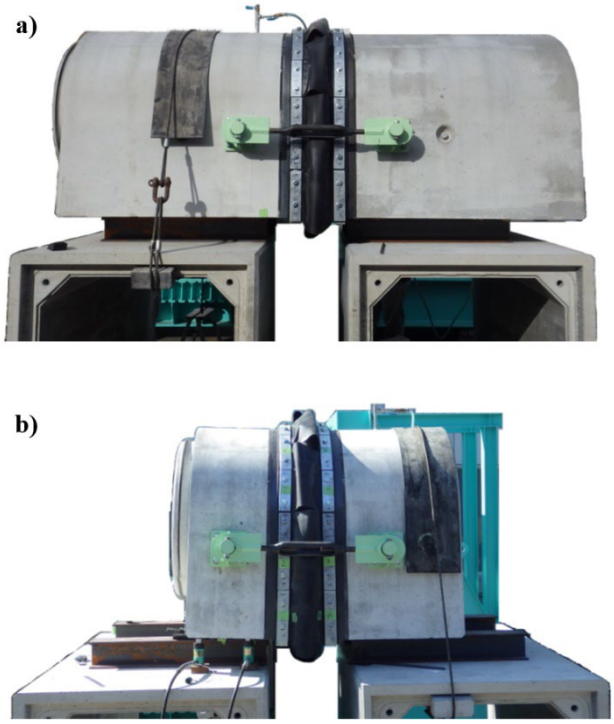

Fig. 19. Watertightness test: a) joints of standard type, and b) central rubber section of highly flexible structure type.

Table 1. Maximum and normalized settlements *S*/*B* of center block.

Stage	Before shaking	After 200 gal	After 300 gal	After 400 gal
Maximum settlement	4.8 mm	27.9 mm	50.2 mm	74.5 mm
Normalized settlement *S*/*B*	1.2×10^{-3}	7.4×10^{-3}	1.3×10^{-2}	2.0×10^{-2}

Table 2. Joint spacing of blocks in watertight test

Types of conduit blocks	Normal installation condition	Elongation condition	Bending condition
Standard type	5 mm	35 mm	Upper side: 10 mm Lower side: 40 mm
Highly flexible structure type	20 mm	70 mm	Upper side: 20 mm Lower side: 70 mm